

Reciprocity in Electron Diffraction and Microscopy

BY A. P. POGANY AND P. S. TURNER

School of Physics, University of Melbourne, Parkville N. 2, Victoria, Australia

(Received 18 April 1967)

The Reciprocity Theorem of scattering theory is shown to hold generally for electrons scattered elastically in an absorbing medium, and also for inelastically scattered electrons, to a certain approximation. Two scattering symmetry conditions are defined by applying the theorem to crystals having mirror symmetry parallel to the crystal surface, and to centrosymmetric crystals. These are general forms of conditions demonstrated by Fukuhara (*J. Phys. Soc. Japan* (1966), **21**, 2645). A number of symmetry effects observable in electron microscope images of crystals result from one or other of these conditions. The variation of intensity of diffracted beams as a function of angular deviation from the Bragg condition is considered in detail. The symmetry of bright-field images of defects lying at equal distances from the crystal surfaces was first explained by Howie & Whelan (*Proc. Roy. Soc.* (1961), **A 263**, 217); such symmetry properties can be conveniently classified and explained by the reciprocity theorem. A method of obtaining high-resolution dark-field images, due to Cowley, is based on the use of the reciprocity theorem. Examples of its application for both Bragg and diffusely scattered electrons are given.

1. Introduction

The Reciprocity Theorem of scattering theory may be stated in terms of two points A, B , and a scatterer, P , as follows:

The amplitude at B of a wave originating from a source at A , and scattered by P , is equal to the scattered amplitude at A due to the same source placed at B .

The theorem was originally used by von Laue (1935) to derive the amplitude outside a crystal due to a point source of X-rays or electrons within it, and hence to obtain the intensities of Kossel and Kikuchi patterns. Von Laue (1948) later generalized the theorem to allow for the production of diffuse scattering from a finite volume of crystal. Kainuma (1955) used this form of the Reciprocity Theorem (R-T) in his theory of Kikuchi patterns. In applying these theories, the two-beam approximation to the dynamical theory was used.

In the usual electron diffraction experiment, both source and point of observation are effectively at infinity, and many diffracted beams are generated simultaneously (n -beam situation). The crystal is assumed to be parallel-sided, with the electrons incident at a small angle to the surface normal. Usually inelastic processes also occur, resulting in electrons being scattered out of the Bragg-diffracted beams. The crystal then acts as an absorber of elastically scattered electrons. We find that none of these conditions restricts the practical application of the R-T to the determination of relations between diffracted intensities.

Before considering the proof of the theorem in § 2 and its implications in electron microscopy, we give an example of the occurrence of the reciprocity effect in an n -beam calculation.

A crystal may often be tilted so that only the line of reflexions nh, nk, nl ($n=0, \pm 1, \pm 2, \dots$) is present in the diffraction pattern. This is the case of 'systematic

reflexions' (Hoerni, 1956). We take the case of a silicon crystal orientated so that the 111 systematics occur, and the Bragg condition for the 111 reflexion is satisfied. The intensity of the conjugate reflexion, $\bar{1}\bar{1}\bar{1}$, is examined as a function of crystal thickness. These initial conditions are shown in Fig. 1(a). Exchange and reversal of the incident and $\bar{1}\bar{1}\bar{1}$ beams results in the conditions given in Fig. 1(b). The theorem says that the intensity of the $\bar{1}\bar{1}\bar{1}$ beam will be the same for both cases, for equal incident intensity. The reciprocal space representation of the two cases is shown in Fig. 1(c). Intensities have been calculated for 100 kV electrons for each case, using the 'multi-slice' method developed by Goodman & Moodie (1965) from the n -beam theory of Cowley & Moodie (1957). The results are given in Figs. 1(d) and 1(e) for some important reflexions. The $\bar{1}\bar{1}\bar{1}$ intensity is the same for both tilts, contrasting strikingly with the gross differences observed for all other reflexions. The same effect is seen in calculations which include absorption coefficients. Intensities obtained experimentally under equivalent conditions show excellent agreement with the computed values (§ 6).

It is not convenient to invert the crystal in a diffraction camera or electron microscope. However, this is found to be unnecessary, since the R-T can be combined with either of two commonly occurring crystal symmetries, thus defining two types of scattering-symmetry condition relating the incident and diffracted beams, and the crystal (§ 3). These are more general forms of relations given by Fukuhara (1966). The use of these relations in interpreting symmetry effects observed in images of perfect and defective crystals is considered in §§ 4 and 5. Finally, we give examples of the use of a recent method of obtaining high-resolution dark-field images (Cowley, 1966), which depends on the reciprocity effect.

2. The reciprocity theorem of scattering theory

The usual proof of the Reciprocity Theorem in scattering theory, involving time-reversal symmetry, assumes an Hermitian Hamiltonian; *i.e.* for potential scattering, a real potential. Such assumption, however, is not necessary for a proof. It is worth noting that the treatment of von Laue (1948) applies equally to a complex potential; see also Bilhorn, Foldy, Thaler, Tobocman & Madsen (1964). Here we present another proof, essentially similar to von Laue's, but which may possibly be more readily visualized and generalized. The treatment is given in terms of scalar quantities, such as electron waves, but analogous theorems hold for vector or spin fields.

Consider a point source of electrons at A . We write Schrödinger's equation in an integral form,

$$\psi(\mathbf{r}) = \frac{\exp(ik|\mathbf{r}-\mathbf{r}_A|)}{|\mathbf{r}-\mathbf{r}_A|} + \int \frac{\exp(ik|\mathbf{r}-\mathbf{r}'|)}{|\mathbf{r}-\mathbf{r}'|} V(\mathbf{r}')\psi(\mathbf{r}')d^3\mathbf{r}',$$

and obtain a Born series by iterating in the usual way:

$$\begin{aligned} \psi(\mathbf{r}) = & \frac{\exp(ik|\mathbf{r}-\mathbf{r}_A|)}{|\mathbf{r}-\mathbf{r}_A|} + \int \frac{\exp(ik|\mathbf{r}-\mathbf{r}'|)}{|\mathbf{r}-\mathbf{r}'|} V(\mathbf{r}') \\ & \frac{\exp(ik|\mathbf{r}'-\mathbf{r}_A|)}{|\mathbf{r}'-\mathbf{r}_A|} d^3\mathbf{r}' + \iint \frac{\exp(ik|\mathbf{r}-\mathbf{r}'|)}{|\mathbf{r}-\mathbf{r}'|} V(\mathbf{r}') \\ & \frac{\exp(ik|\mathbf{r}'-\mathbf{r}''|)}{|\mathbf{r}'-\mathbf{r}''|} V(\mathbf{r}'') \frac{\exp(ik|\mathbf{r}''-\mathbf{r}_A|)}{|\mathbf{r}''-\mathbf{r}_A|} \\ & d^3\mathbf{r}'d^3\mathbf{r}'' + \dots \end{aligned}$$

Now interchanging \mathbf{r} and \mathbf{r}_A does not change the value of any of the terms. Pictorially, one can imagine a scattering process of any order proceeding from A via points \mathbf{r}' , \mathbf{r}'' , ..., to \mathbf{r} , and the reciprocal process from \mathbf{r} via ..., \mathbf{r}'' , \mathbf{r}' , to A , 'matching' the first exactly in potential and propagation terms. V need not be real; the essential element is the symmetry of the Green's function. One notes incidentally that reciprocity holds for each term of the Born series separately.

For inelastic scattering, the time-reversal approach requires the scatterer to be in its excited state for the reciprocal process. This is not suitable for the present applications; we wish to consider the scatterer starting always in its ground state (or thermal equilibrium, as appropriate). In this case, one can derive a reciprocity theorem under suitable restrictions.

We use the theory and notation of Yoshioka (1957), in which scattering (not necessarily by a crystal) is described by a set of coupled equations. Neglecting constants, these are:

$$\nabla^2\varphi_n + k_n^2\varphi_n = \sum_m H'_{nm}\varphi_m, \quad n=0,1,2,\dots$$

$n=0$ represents the elastically scattered wave. Each equation can be expanded in a Born series, but only

the $n=0$ equation has a leading term, representing the incident wave. For a given φ_n , each iteration after the first includes contributions from all φ .

Writing

$$G_n(\mathbf{r},\mathbf{r}') \equiv \frac{\exp(ik_n|\mathbf{r}-\mathbf{r}'|)}{|\mathbf{r}-\mathbf{r}'|}$$

one has

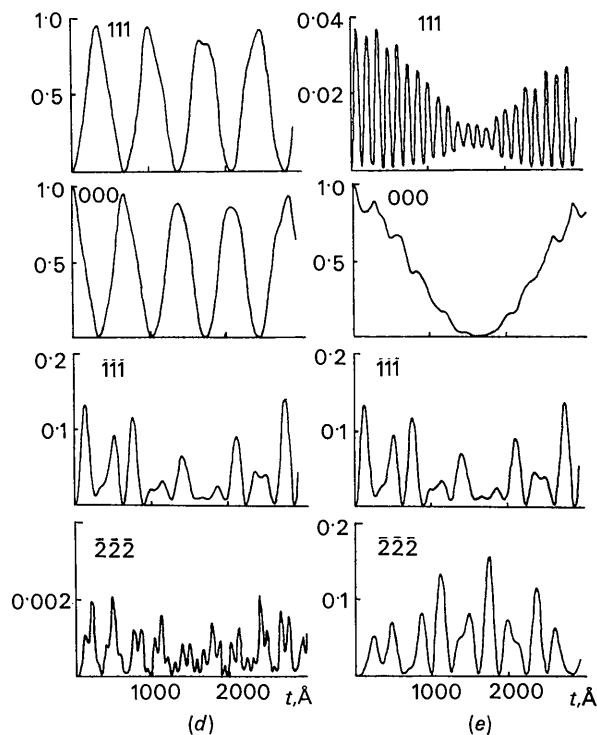
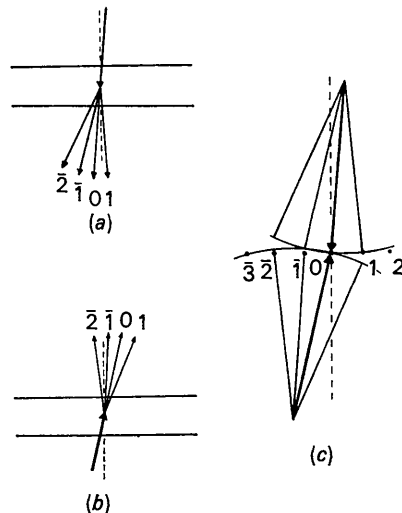


Fig.1. Reciprocity effect in intensities for silicon 111-systematic reflexions, computed as functions of thickness, t . (21-beam calculation). (a) Bragg condition for 111 satisfied giving intensities shown in (d); application of R-T for 111 reflexion exchanges and reverses incident and 111 beams, as in (b); the 333 Bragg condition is now satisfied. (e) All intensities except the 111 are different. Ewald sphere construction (c) emphasizes changes in excitation errors for all reflexions.

$$\varphi_n(\mathbf{r}) = \int G_n(\mathbf{r}, \mathbf{r}') H'_{n0}(\mathbf{r}') G_o(\mathbf{r}', \mathbf{r}_A) d\mathbf{r}' + \iint G_n(\mathbf{r}, \mathbf{r}') \sum_m H'_{nm}(\mathbf{r}') G_m(\mathbf{r}', \mathbf{r}'') H'_{m0}(\mathbf{r}'') G_o(\mathbf{r}'', \mathbf{r}_A) d\mathbf{r}' d\mathbf{r}'' + \dots,$$

with obvious physical interpretation. Now if one makes the (usual) assumption $k_n \simeq k_o$ for all processes contributing significantly to the scattered intensity, the functions G_m can be taken out of the summations. By definition,

$$H'_{nm}(\mathbf{r}) = \int a_n^*(\mathbf{q}) V(\mathbf{q}, \mathbf{r}) a_m(\mathbf{q}) d\mathbf{q},$$

where $V(\mathbf{q}, \mathbf{r})$, (H' in Yoshioka's paper), is the interaction energy between the incident electron (coordinate \mathbf{r}) and the scatterer (coordinates \mathbf{q}). Furthermore the states $a_n(\mathbf{q})$ of the scatterer form a complete orthonormal set, for which the closure property holds;

$$i.e. \quad \sum_m a_m^*(\mathbf{q}') a_m(\mathbf{q}) = \delta(\mathbf{q}' - \mathbf{q}).$$

Hence

$$\begin{aligned} \sum_m H'_{nm}(\mathbf{r}) H'_{mp}(\mathbf{r}') &= \sum_m \int a_n^*(\mathbf{q}) V(\mathbf{q}, \mathbf{r}) a_m(\mathbf{q}) d\mathbf{q} \int a_m^*(\mathbf{q}') \\ &\times V(\mathbf{q}', \mathbf{r}') a_p(\mathbf{q}') d\mathbf{q}' = \int a_n^*(\mathbf{q}) V(\mathbf{q}, \mathbf{r}) V(\mathbf{q}, \mathbf{r}') a_p(\mathbf{q}) d\mathbf{q}. \end{aligned}$$

So one obtains, for the integrand of a term in the Born series, a product of the G 's and an integral

$$\int a_n^*(\mathbf{q}) V(\mathbf{q}, \mathbf{r}') V(\mathbf{q}, \mathbf{r}'') \dots V(\mathbf{q}, \mathbf{r}''') a_o(\mathbf{q}) d\mathbf{q},$$

which depends only on the initial and final states of the scatterer and on the positions \mathbf{r}' , \mathbf{r}'' , ... of the scattering, but not on their order. So all the symmetry required for a proof of the R-T by the previous method is present here, subject only to the above approximation.

To include all inelastic (and thermal) processes which scatter in a given direction, one simply notes that they are incoherent if they leave the scatterer in a different state. Then there results a reciprocity of intensities.

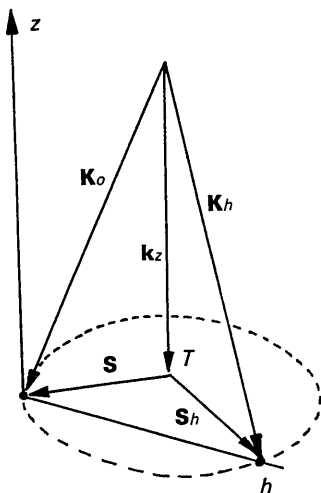


Fig. 2. Definition of T , \mathbf{k}_z , \mathbf{s} , and \mathbf{s}_h .

The validity of the process of taking both \mathbf{r}_A and \mathbf{r} to infinity has been considered by Bilhorn *et al.* (1964).

3. The reciprocity theorem and crystal symmetry

The R-T enables one to find two incident beam directions for which the amplitudes of a given diffracted beam are equal. However, the electrons are incident on opposite faces of the crystal. Two types of scattering-symmetry condition are defined, relating amplitudes of diffracted beams *via* the R-T and a crystal symmetry operation. Type I involves reflexion in a crystal plane, and type II involves a central inversion.

The crystal, of thickness t , is represented by the symbol C ; the mirror image of this in the plane $z=t/2$, mid-way between the surfaces, is the crystal $C^{(m)}$. Likewise, the crystal C^- is the result of inversion of crystal C^+ in its centre.

A notation similar to Fukuhara's (1966) is used: $\psi_h(\mathbf{k}_z, \mathbf{s}, C)$ represents the amplitude of the reflexion from the crystal C , \mathbf{k}_z and \mathbf{s} being the components of the incident wave-vector along, and perpendicular to the surface normal, z , respectively. Then the R-T is expressed by

$$\psi_h(\mathbf{k}_z, \mathbf{s}, C) = \psi_h(-\mathbf{k}_z, -(\mathbf{s} + \mathbf{h}), C), \quad (3.1)^*$$

since \mathbf{s}_h , the component of the diffracted wave-vector perpendicular to z , is given by

$$\mathbf{s}_h = \mathbf{s} + \mathbf{h} \text{ (see Fig. 2).}$$

By putting $\mathbf{s} = -\mathbf{h}/2 + \mathbf{r}$ in (3.1), and reflecting the r.h.s. in the plane $z=t/2$, we obtain the relation between diffracted waves in C and $C^{(m)}$:

Type I:

$$\psi_h(\mathbf{k}_z, -\mathbf{h}/2 + \mathbf{r}, C) = \psi_h(\mathbf{k}_z, -\mathbf{h}/2 - \mathbf{r}, C^{(m)}). \quad (3.2)$$

Similarly, by inversion of the r.h.s. of (3.1) in the centre of crystal C^+ , we obtain

Type II:

$$\psi_h(\mathbf{k}_z, -\mathbf{h}/2 + \mathbf{r}, C^+) = \psi_{\bar{h}}(\mathbf{k}_z, -\mathbf{h}/2 - \mathbf{r}, C^-). \quad (3.3)$$

Hence type I relation holds for a crystal mirror-symmetric about the plane $z=t/2$ ($C^{(m)} = C$), and type II holds for a centrosymmetric crystal ($C = C^+ = C^-$). Strictly speaking, the symmetry should be satisfied by (i) the crystal symmetry, (ii) the crystal boundaries, and (iii) the crystal defects, if present. However, frequently one or other of these may be relaxed; for example, use of the 'column approximation' allows one to neglect the exact form of the surfaces. Again, if one considers only the zero layer of the reciprocal lattice ($l=0$), mirror symmetry about $z=t/2$ always holds close to the

* It should be noted that in this and similar equations, the notation \mathbf{k}_z or $-\mathbf{k}_z$ is used only to indicate whether the electron beam is incident from above or below the crystal. No relation between the magnitudes of the \mathbf{k}_z 's appearing on either side of the equations is implied, since this is determined by \mathbf{s} or $\mathbf{s} + \mathbf{h}$ respectively. The authors are grateful to Mr A. F. Moodie for pointing this out.

principal orientation, and for a single row of $hk0$ systematic reflexions it holds for any orientation.

Fukuhara (1966) has derived symmetry relationships between intensities of diffracted beams, from the properties of the scattering matrix for a centrosymmetric crystal. Our equations (3.3), (3.2) are the amplitude forms of his equations (18), (20) respectively.

It is often useful to be able to state the above equations in diagrammatic form. The diffracting conditions are specified by the projection T of the tie-point on the $hk0$ reciprocal lattice plane, (Fukuhara, 1966). The arrow notation is used to show the direction of \mathbf{k}_z . In Fig. 3 the R-T and type II conditions are shown.

A real-space diagram is useful when only systematic reflexions are considered. Type I symmetry is illustrated in Fig. 4, where the directions of the (unit-amplitude) incident wave and of ψ_h are specified by angles α, β to the surface normal, mm' is the mirror plane, and θ the Bragg angle.

Finally, it should be noted that equations (3.1)–(3.3) imply no restrictions on the number of beams interacting, other than the limitations imposed if only systematic or $hk0$ interactions are considered.

4. Symmetry in images of perfect crystals

By 'perfect' crystals, we mean those containing no defects resolvable in electron microscope images. When considering images of bent or wedge shaped crystals, we assume the column approximation to hold*.

4.1 Dark-field rocking curves

Rocking curves – the variation of intensity with angle of incidence – can be obtained experimentally by dark-field imaging of bent crystals of uniform thickness, and by the convergent beam technique (Goodman & Lehmpfuhl, 1965). We assume the presence of a mirror plane, or neglect hkl interactions for $l \neq 0$. Type I symmetry conditions then apply. The intensity of the h rocking curve may be plotted as a function of the components $s_{\parallel h}, s_{\perp h}$ of \mathbf{s} in the directions parallel and perpendicular to \mathbf{h} . We define the *principal Bragg orientation* $P(h)$ for the reflexion h to be that for which $\mathbf{s} = -\mathbf{h}/2$. By application of equation (3.2) we see that the intensity in the rocking curve of points related by inversion through P are equal [e.g. (J, J') or (I, I') in Fig. 5(a)].

When the crystal is tilted about the \mathbf{h} direction until only the systematic reflexions $n\mathbf{h}$, ($n=0, \pm 1, \dots$), have significant amplitude, scattering occurs only in the plane defined by the incident wave-vector \mathbf{K}_0 and \mathbf{h} . Under these conditions, the rocking curve becomes a function of $s_{\parallel h}$ only, and is symmetrical about the Bragg position ($s_{\parallel h} = h/2$). This can be seen by studying Fig. 4; we have $\alpha + \beta = 2\theta$, and hence if $\alpha = \theta + \Delta\theta$, then $\beta = \theta - \Delta\theta$.

Intensities at points I, J in Fig. 5(a) will not be equal in general because of the presence of non-systematic interactions. In practical cases, other symmetry elements of the crystal (e.g. a mirror plane) will often cause equality of intensities at J and I' , and hence at J and I . Fukuhara's (1966) statement that the h bend contour is 'symmetric with respect to a line passing along the h th Bragg position' is correct only if such additional conditions are present, or if non-systematic reflexions are absent.

The convergent beam technique provides a most sensitive means of observing symmetries in angular distribution of scattering from the crystal (see Goodman & Lehmpfuhl, 1965). A convergent beam pattern of hexagonal cadmium sulphide close to $1\bar{1}0$ orientation was taken* so that the 004, 220 and 224 reflexions were all satisfied simultaneously for a direction close to the axis of the cone of illumination. Then the point $P(224)$ lies in the 224 disc, and the symmetry of intensity about this point is evident [see Fig. 5(b)]. The (110) plane in cadmium sulphide is a plane of mirror symmetry. Thus points I, J [Fig. 5(a)] will have equal intensity for the 00 l reflexions, as is seen in the 004 disc of Fig. 5(b).

* This convergent beam pattern was taken by Mr P. Goodman on the convergent beam diffraction camera of Cockayne, Goodman, Mills & Moodie (1967) at C.S.I.R.O. Division of Chemical Physics, Clayton, Victoria.

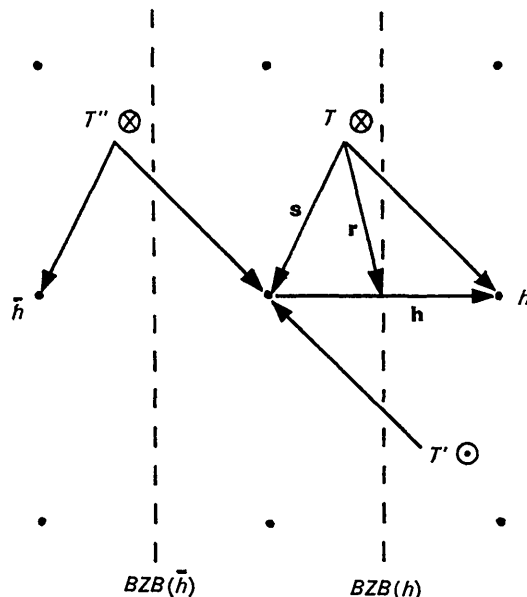


Fig. 3. Reciprocal space diagram representing terms of equations (3.1) and (3.2) in the $hk0$ reciprocal lattice plane.

Point	Incident vector	Scattering expression
$T \otimes$	$+\mathbf{k}_z, \mathbf{s}$	$\psi_h(\mathbf{k}_z, \mathbf{s}, C^+)$
$T' \circ$	$-\mathbf{k}_z, -(\mathbf{s} + \mathbf{h})$	$\psi_h(-\mathbf{k}_z, -(\mathbf{s} + \mathbf{h}), C^+)$
$T'' \otimes$	$+\mathbf{k}_z, (\mathbf{s} + \mathbf{h})$	$\psi_{\bar{h}}(\mathbf{k}_z, (\mathbf{s} + \mathbf{h}), C^-)$

If T lies on the h -Brillouin zone boundary [BZB(h)], then the Bragg condition for h is satisfied.

* The column approximation was introduced by Hirsch, Howie & Whelan (1960).

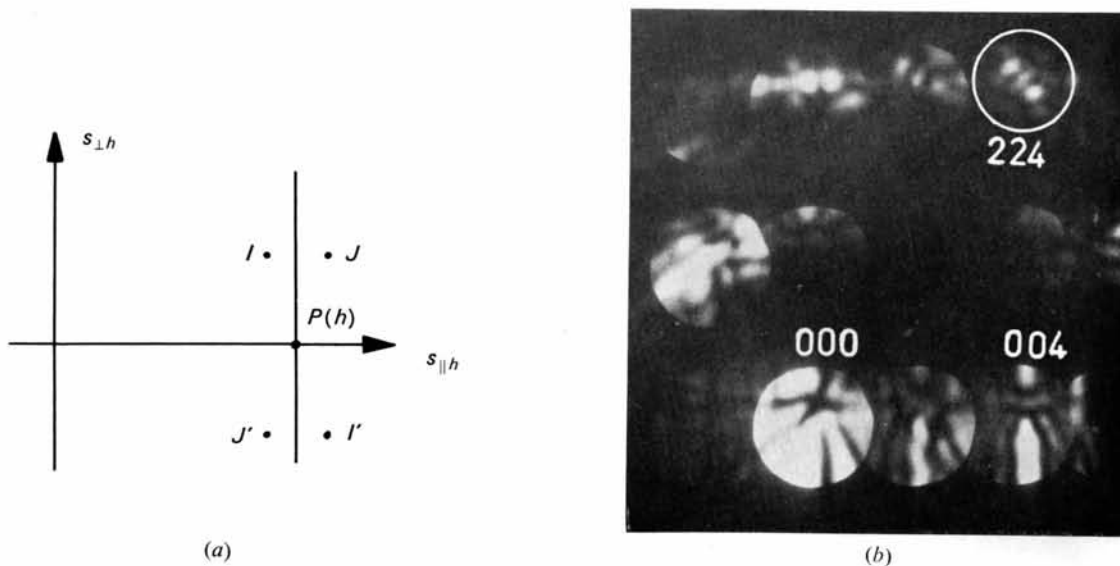


Fig. 5. Symmetry of rocking curves for the reflexion h about the principal Bragg orientation, $P(h)$. (a) Definition of $P(h)$ and equivalent points (I, I') and (J, J') in plot of intensity of reflexion h as a function of incident beam direction s . (b) Convergent beam pattern from cadmium sulphide, showing symmetry of intensity of 224 beam about $P(224)$, and symmetry of 004 intensity across the line $s_{\parallel[004]} = \frac{1}{2}[004]$. $P(224)$ is the centre of the circle drawn about the 224 disc.

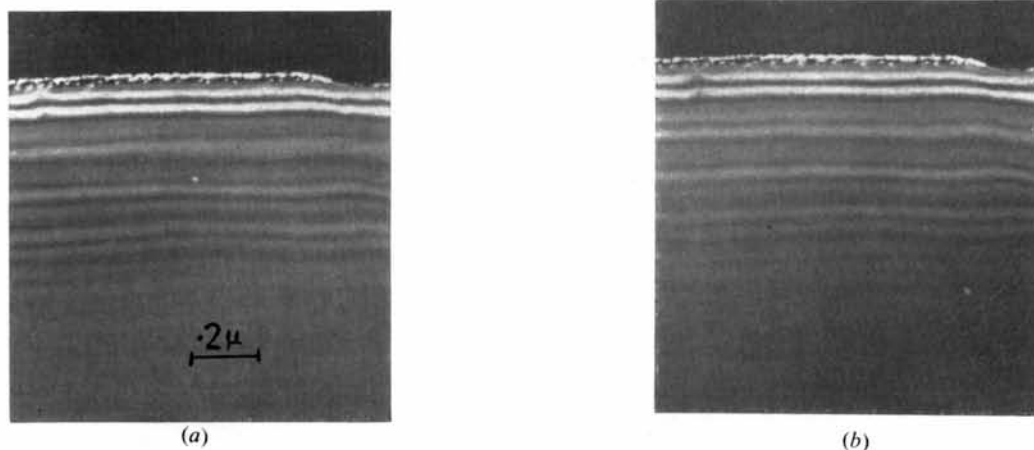


Fig. 6. Thickness extinction contours in silicon wedge, tilted to satisfy the 111 systematics. (a) $\bar{1}\bar{1}\bar{1}$ translated aperture dark field image, for 111 Bragg condition satisfied; (b) corresponding HRDF image; *i.e.* 111 image for the 333 Bragg condition satisfied. Compare with Fig. 1.

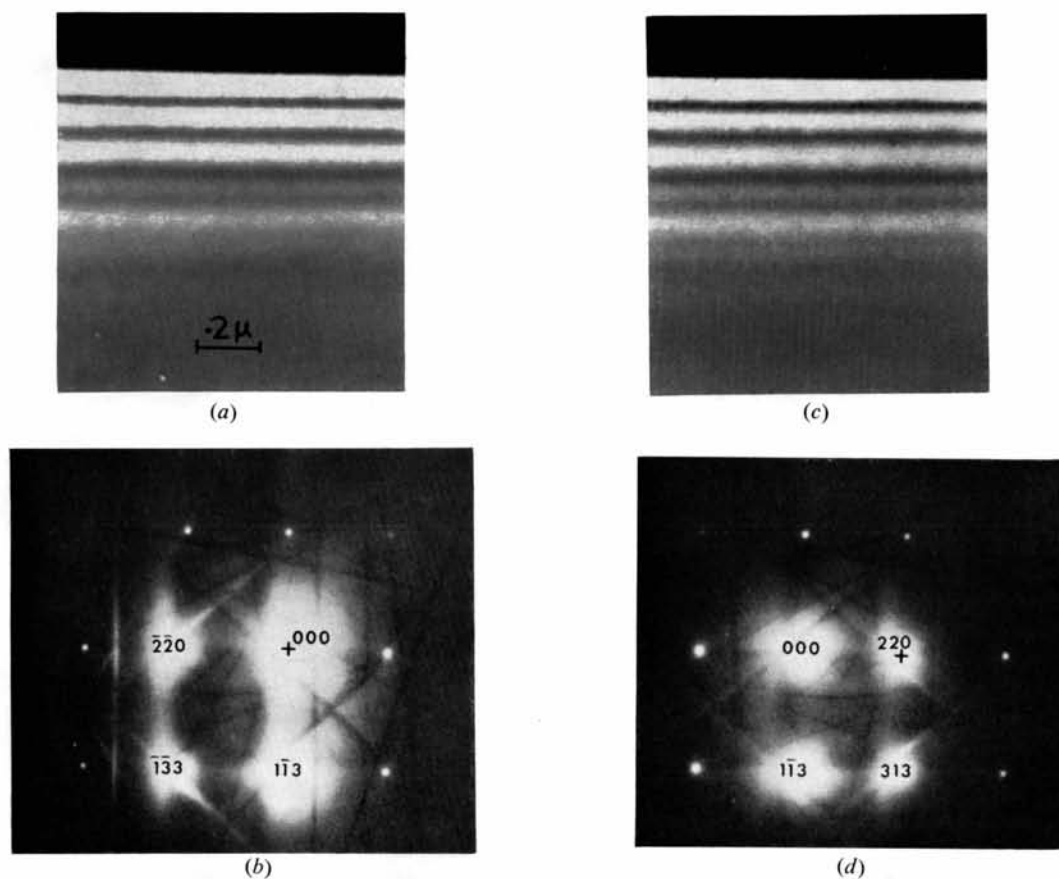


Fig. 7. Images of silicon wedge close to $[3\bar{3}2]$ orientation. (a) Translated-aperture $\bar{2}20$ dark field image, for diffraction conditions shown in (b). (c) HRDF 220 image, after beam had been tilted through $-2\theta_{\bar{2}20}$ to place 220 on the optic axis (marked +), leading to diffraction conditions shown in (d).

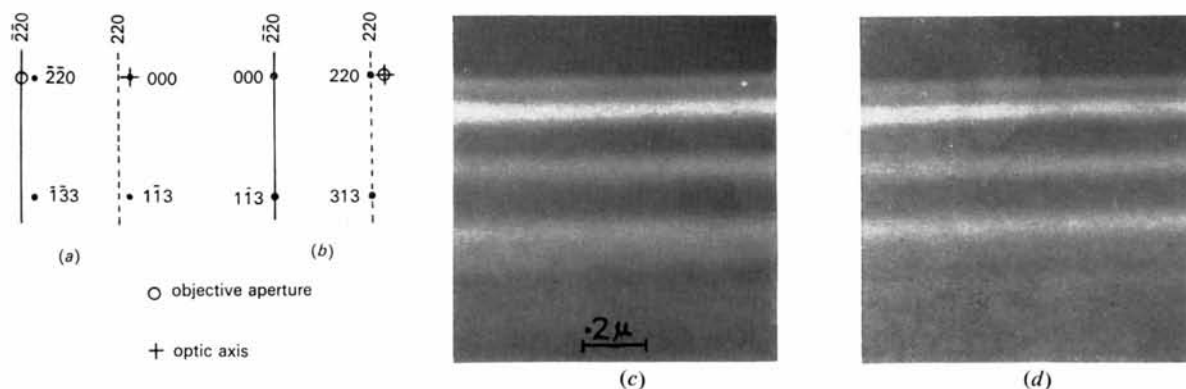


Fig. 8. Images of $[3\bar{3}2]$ silicon wedge obtained with inelastically scattered electrons. (a) With the beam initially untilted, the 5μ objective aperture was placed on the $\bar{2}20$ Kikuchi line, close to the $\bar{2}20$ spot, giving the image (c). (b) The beam was tilted to place the 000 spot on the $\bar{2}20$ Kikuchi line, thus satisfying the HRDF tilt condition for the selected diffuse scattering angle. The aperture was placed on the optic axis, giving the image shown in (d).

4.2 Symmetry of bright-field images

Equation (3.3) gives for $h=0$

$$\psi_o(\mathbf{k}_z, \mathbf{s}, C^+) = \psi_o(\mathbf{k}_z, \mathbf{s}, C^-). \quad (4.1)$$

Adjacent 180° domains in ferroelectric BaTiO_3 are related by central inversion, *i.e.* they are relative C^+ , C^- crystals. An excellent experimental example of (4.1) is observable in the bright-field micrographs of BaTiO_3 , 180° domains given by Tanaka & Honjo (1966). Intensities in the perfect crystal parts of the domains (*i.e.* away from the boundaries) are equal for constant thickness. This result has been obtained for the two-beam case by Gevers, Blank & Amelinckx (1966).

When type I symmetry is present, equation (3.2) gives for the main beam

$$\psi_o(\mathbf{k}_z, \mathbf{s}, C) = \psi_o(\mathbf{k}_z, -\mathbf{s}, C). \quad (4.2)$$

Thus bright-field intensities for a non-centrosymmetrical crystal are identical for equal tilts $\pm \mathbf{s}$. This has been observed in convergent beam patterns of cadmium sulphide (Goodman, 1966; Goodman & Lehmpfuhl, 1967). An alternative interpretation has been given by Moodie (1967), in terms of the scattering diagrams introduced by Gjønnes & Moodie (1965).

5. Symmetry of defect images

Theories of the contrast of crystal defects imaged in the electron microscope are commonly based on the column approximation*. The deviation from perfection of the lattice in a column near the defect is described by a function $\mathbf{R}(z)$ of the depth z in the column, of thickness t . \mathbf{R} is usually, but not necessarily, a displacement parameter (Gevers, van Landuyt & Amelinckx, 1965; Amelinckx, 1965). Only the component of a displacement $\mathbf{R}(z)$ parallel to the imaging reflexion vector \mathbf{h} (and thus perpendicular to z) contributes to the image intensity†, and hence need be considered in

* See footnote on previous page.

† Reviews of the theories of defect image contrast have been given by Amelinckx (1964) and by Hirsch, Howie, Nicholson, Pashley & Whelan (1965).

applying the symmetry relations to prediction of image intensity.

Columns in different parts of a crystal containing defects are often related by one of the following two types of symmetry. The corresponding diffraction symmetry then applies, leading to equality of intensity from these columns.

Type I: $\mathbf{R}_1(z) = \mathbf{R}_2(t-z)$. Columns 1,2 related by mirror inversion in the plane $z=t/2$.

Dark-field images of crystal regions in or near defects, for which this relation holds, will be identical if the Bragg angle is satisfied, and systematic interactions occur. The crystal need not be centrosymmetric. Ball (1964) has proved equality of intensities from columns for which $\mathbf{R}(z) = \mathbf{R}_0 + \mathbf{R}(t-z)$, provided the Bragg angle is satisfied under two-beam conditions. The addition of the constant \mathbf{R}_0 does not change the image intensity. Type I symmetry also holds for the δ -boundaries of Gevers *et al.* (1965), for which the displacement in the second region is a linear function of thickness (see Amelinckx, 1965).

Type II: $\mathbf{R}_1(z) = -\mathbf{R}_2(t-z)$. Columns 1,2 related by central inversion.

Bright-field images of regions in or near defects for which this holds will be identical for any incident beam direction. The crystal must be centrosymmetric, but one is not limited to systematic interactions. This result is equivalent to that of Howie & Whelan (1961), who showed by matrix methods that 'bright-field images of crystals with displacements $\mathbf{R}(z)$ and $\mathbf{R}_0 - \mathbf{R}(t-z)$ are identical'. This is the case for stacking fault fringes, and the α -boundaries of Gevers *et al.* (1965). The 'pseudo anti-symmetry' of dark-field fringe patterns of stacking faults (Gevers *et al.*, 1965) is a further example of type II symmetry.

6. High-resolution dark-field microscopy

Although the advantages of the high-resolution dark-field technique (HRDF) over the translated-aperture method have been recognized for a number of years

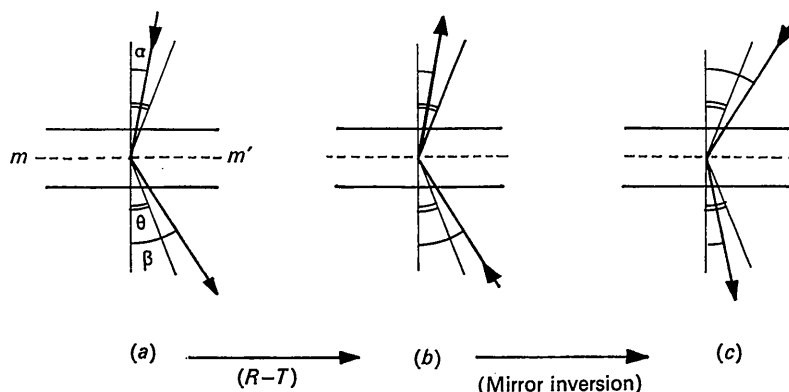


Fig. 4. Real space illustration of type I scattering symmetry between diffraction conditions shown in (a) and (c).

(Pashley & Presland, 1958), the lack of efficient beam-tilting and anti-contamination devices has, until very recently, prevented its application. (For a recent review, see Hirsch *et al.*, 1965). However, a number of microscopes are now available with electromagnetic beam-tilting, and excellent anti-contamination attachments, and the HRDF method is becoming popular (Hale & McLean, 1964).

The technique normally consists in tilting the incident beam until the required diffracted beam, h , is directed down the optic axis, and then tilting the crystal to obtain the desired diffraction condition (see *e.g.* Alderson & Halliday, 1965). An alternative method, (Cowley, 1966), has considerable advantages, especially for centrosymmetric crystals. The untilted beam is assumed to be aligned on the optic axis, and the crystal orientation set to the desired diffraction condition for the reflexion h . Then to obtain a HRDF image for h , the beam is tilted until the conjugate reflexion, \bar{h} , is aligned on the optic axis, and the image recorded*.

We can represent the two cases by:

$$\text{Initial: } I_h(\mathbf{k}_z, \mathbf{s}, C); \quad \text{Tilted: } I_{\bar{h}}(\mathbf{k}_z, \mathbf{s} + \mathbf{h}, C).$$

If the crystal is centrosymmetric, it follows from equation (3.3) that these expressions are equal,

$$\text{i.e.} \quad I_h(\mathbf{k}_z, \mathbf{s}, C) = I_{\bar{h}}(\mathbf{k}_z, \mathbf{s} + \mathbf{h}, C). \quad (6.1)$$

This is shown in Fig. 3. Then the HRDF image for \bar{h} obtained by this method is identical with the required image for h observable by the translated-aperture technique, except that it lacks the aberrations inherent in off-axis images. In bringing the conjugate reflexion to the optic axis, the beam is tilted through an angle $-2\theta_h$, corresponding to the translation \mathbf{h} of all spots in the diffraction pattern. Cowley (1966) has pointed out that repeated application of the method to successive beams would allow one to obtain the diffraction pattern from an area of the crystal only a few times larger than the smallest resolvable by the microscope.

To obtain a HRDF image for the reflexion h of a non-centrosymmetric crystal which is initially at orientation $+\mathbf{s}$, the crystal must be tilted to orientation $-\mathbf{s}$, and the beam tilted to position the reflexion h on the optic axis. Type I symmetry is assumed to hold.

To see that this is so, we look for a HRDF condition equivalent to the initial condition

$$I_h(\mathbf{k}_z, +\mathbf{s}, C). \quad (6.2)$$

Since type I symmetry is present, a condition equivalent to (6.2) may be found by applying equation (3.2), which gives

$$I_h(\mathbf{k}_z, -(\mathbf{s} + \mathbf{h}), C). \quad (6.3)$$

The diffracted beam h is required to be directed down the optic axis. The vector \mathbf{s}_h specifying this direction is given by

$$\mathbf{s}_h = -(\mathbf{s} + \mathbf{h}) + \mathbf{h} = -\mathbf{s}.$$

Hence $-\mathbf{s}$ must specify the optic axis, and thus the crystal must be tilted to orientation $-\mathbf{s}$.

This HRDF technique for centrosymmetric crystals has proved in practice to be fast and accurate. A JEM-7A fitted with the JEM-ABD2 beam-tilting device (Yanaka, Watanabe & Hirai, 1966), a precision goniometer stage (Honjo, 1962), and an efficient anti-contamination device, was used to study wedges of silicon at 100 kV. Two examples are presented here.

Intensity variation of $\bar{111}$ thickness contours closely comparable to the computed values given in Fig. 1(*d, e*), was obtained from a wedge tilted to give 111 systematic reflexions under the diffracting conditions defined in Fig. 1(*a, b*). The images are shown in Fig. 6.

Another silicon wedge was tilted close to the $[3\bar{3}2]$ orientation, so that many reflexions had significant intensity. The comparison of the translated-aperture $\bar{220}$, and high-resolution $\bar{220}$ images is given in Fig. 7.

Some diffusely scattered electrons will always pass the objective aperture, and be included in a normal electron microscope image. The reciprocity theorem should hold for these electrons, as shown in § 2, provided the wavelength change can be neglected. Equation (6.1) still holds, except that \mathbf{h} is now considered to be a continuous function specifying the angle for the inelastic electrons. In principle, a vanishingly small objective aperture should be used when testing the R-T for diffuse scattering.

Experimental evidence for the validity of the R-T for diffuse scattering was obtained, with use of the same silicon wedge. A 5μ objective aperture was used in imaging diffuse electrons near the $\bar{220}$ Bragg spot, by displacing the aperture (Kamiya & Uyeda, 1961). The $\bar{220}$ Kikuchi line passed through the region selected [Fig. 8(*a*)]. The beam was then tilted to place the 000 spot on the selected position on the $\bar{220}$ Kikuchi line, and the corresponding image taken with the aperture on the optic axis, as shown in Fig. 8(*c*). The two diffuse images agree well [Figs. 8(*c, d*)], although microphotometry of these and similar pairs of images reveals differences in the background intensities, and fringe contrast. Since the aperture diameter was as great as one-sixth of the spot separation, detailed agreement is not expected. It is thought that some of the differences may be due to inelastically scattered electrons for which the wavelength change cannot be neglected, but experiments using an energy analyser would be necessary to confirm this.

We thank Professor J. M. Cowley and Dr A. E. C. Spargo for many constructive comments on this work, and Mr P. Goodman for taking convergent beam patterns, and for permission to include the one used in Fig. 5(*b*). The work was supported by a grant from the Australian Research Grants Committee.

The financial support of Commonwealth Post-Graduate Awards is gratefully acknowledged.

* If, under HRDF conditions, the Bragg conditions for h are satisfied, then the conjugate beam \bar{h} will be satisfied for zero beam tilt. This was pointed out by Hale (see Alderson & Halliday, 1965).

References

- ALDERSON, R. H. & HALLIDAY, J. S. (1965). In *Techniques for Electron Microscopy*, ed. D. H. Kay, 2nd. edn. Oxford: Blackwell.
- AMELINCKX, S. (1964). *Solid State Physics*, Supplement 6. New York: Academic Press.
- AMELINCKX, S. (1965). *Int. Conf. Electron Diff. and Cryst. Defects, Melbourne, J-1* (Abstract).
- BALL, C. J. (1964). *Phil. Mag.* **9**, 541.
- BILHORN, D. E., FOLDY, L. L., THALER, R. M., TOBOCMAN, W. & MADSEN, V. A. (1964). *J. Math. Phys.* **5**, 435.
- COCKAYNE, D. J. H., GOODMAN, P., MILLS, J. C. & MOODIE, A. F. (1967). *Rev. Sci. Instrum.* **38**, 1097.
- COWLEY, J. M. (1966). Summer School on Dynamical Theory of Diffraction, Harmonia, Czechoslovakia. To be published in *Acta Universitatis Comenia Geologica*.
- COWLEY, J. M. & MOODIE, A. F. (1957). *Acta Cryst.* **10**, 609.
- FUKUHARA, A. (1966). *J. Phys. Soc. Japan*, **21**, 2645.
- GEVERS, R., BLANK, H. & AMELINCKX, S. (1966). *Phys. Stat. Sol.* **13**, 449.
- GEVERS, R., VAN LANDUYT, J. & AMELINCKX, S. (1965). *Phys. Stat. Sol.* **11**, 689.
- GJØNNES, J. & MOODIE, A. F. (1965). *Acta Cryst.* **19**, 65.
- GOODMAN, P. (1966). 6th. *Int. Congress Electron Microscopy, Kyoto. Abstracts*, **1**, 57. Tokyo: Maruzen Co.
- GOODMAN, P. & LEHMPFUHL, G. (1965). *Z. Naturforsch.* **20a**, 110.
- GOODMAN, P. & LEHMPFUHL, G. (1967). *Acta Cryst.* Submitted for publication.
- GOODMAN, P. & MOODIE, A. F. (1965). *Int. Conf. Electron Diff. and Cryst. Defects, Melbourne. 1D-1, 1D-2.* (Abstract.)
- HALE, K. F. & MCLEAN, D. (1964). *Nature, Lond.* **201**, 696.
- HIRSCH, P. B., HOWIE, A., NICHOLSON, R. B., PASHLEY, D. W. & WHELAN, M. J. (1965). *Electron Microscopy of Thin Crystals*. London: Butterworths.
- HIRSCH, P. B., HOWIE, A. & WHELAN, M. J. (1960). *Phil. Trans. A*, **252**, 499.
- HOERNI, J. (1956). *Phys. Rev.* **102**, 1534.
- HONJO, G. (1962). *J. Phys. Soc. Japan*, **17**, Supp. B-II, 277.
- HOWIE, A. & WHELAN, M. J. (1961). *Proc. Roy. Soc. A*, **263**, 217.
- KAINUMA, Y. (1955). *Acta Cryst.* **8**, 247.
- KAMIYA, Y. & UYEDA, R. (1961). *J. Phys. Soc. Japan*, **16**, 1361.
- LAUE, M. VON (1935). *Ann. Phys. Lpz.* **23**, 705.
- LAUE, M. VON (1948). *Materiewellen und ihre Interferenzen*. Leipzig: Akad. Verl.
- MOODIE, A. F. (1967). To be published.
- PASHLEY, D. W. & PRESLAND, A. E. B. (1958). *J. Inst. Metals*, **87**, 419.
- TANAKA, M. & HONJO, G. (1966). 6th *Int. Congress Electron Microscopy, Kyoto. Abstracts* **1**, 83. Tokyo: Maruzen Co.
- YANAKA, T., WATANABE, M. & HIRAI, T. (1966). 6th *Int. Congress Electron Microscopy, Kyoto, Abstracts*, **1**, 185. Tokyo: Maruzen Co.
- YOSHIOKA, H. (1957). *J. Phys. Soc. Japan*, **12**, 618.

Acta Cryst. (1968). A **24**, 109

Diffuse Scattering in Electron Diffraction Patterns.

I. General Theory and Computational Methods

BY J. M. COWLEY AND A. P. POGANY

School of Physics, University of Melbourne, Parkville N.2, Victoria, Australia

(Received 16 January 1967 and in revised form 5 June 1967)

The solution of the n -beam dynamical theory of the diffraction of electrons by crystals is generalized to cover the case of diffraction by crystals containing defects and disorders, including thermal motion. The conditions and assumptions under which practical computer calculations of diffuse intensities can be made are explored on the basis of the slice approach of Goodman and Moodie, although matrix methods are equally applicable. It is shown that, if the range of correlation of the deviations from the perfect crystal lattice is small, the total diffuse scattering can be expressed in terms of dynamical factors which multiply the intensities calculated using the kinematical approximation. Simple expressions are derived for the absorption coefficients which must be applied to the sharp Bragg reflexions to take account of the energy lost from them into the diffuse scattering. The possibility that the intensity of diffuse scattering may show dependence on the range of correlation of the defects is discussed.

1. Introduction

Especially since improved techniques have made it possible to observe single-crystal spot patterns from very small single crystals, a great many observations have been made of diffuse scattering effects in electron diffraction patterns, arising from thermal motion of the atoms and various types of defects and disorder in the crystal. In many cases these observations parallel those made on single crystals by X-ray diffraction methods,

but the relative ease of observation of the effects in electron diffraction patterns, the possibility of using extremely small crystals, and the increasing evidence for effects not directly comparable with those familiar from X-ray work are all factors which suggest that a sound basis for the interpretation of the observed intensities would be of great value.

Following the initial work of Yoshioka (1957), concerning the effects of inelastic diffuse-scattering processes, a number of authors have reported theoretical